Light-Emitting Diodes Hot Paper

International Edition: DOI: 10.1002/anie.201504791
German Edition: DOI: 10.1002/ange.201504791

Waterproof Alkyl Phosphate Coated Fluoride Phosphors for Optoelectronic Materials

*Hoang-Duy Nguyen, Chun Che Lin, and Ru-Shi Liu**

Abstract: *A facile approach for coating red fluoride phosphors with a moisture-resistant alkyl phosphate layer with a thickness of 50–100 nm is reported. $K_2SiF_6:Mn^{4+}$ particles were prepared by co-precipitation and then coated by esterification of P_2O_5 with alcohols (methanol, ethanol, and isopropanol). This route was adopted to encapsulate the prepared phosphors using transition-metal ions as cross-linkers between the alkyl phosphate moieties. The coated phosphor particles exhibited a high water tolerance and retained approximately 87 % of their initial external quantum efficiency after aging under high-humidity (85 %) and high-temperature (85 °C) conditions for one month. Warm white-light-emitting diodes that consisted of blue InGaN chips, the prepared $K_2SiF_6:Mn^{4+}$ phosphors, and either yellow $Y_3Al_5O_{12}:Ce^{3+}$ phosphors or green β-SiAlON: Eu^{2+} phosphors showed excellent color rendition.*

Narrow-band red-emitting fluoride phosphors doped with manganese(IV) have recently attracted increasing attention for applications in warm white-light-emitting diodes (WLEDs) because of their optical properties, thermal stability, and feasible preparation.[1–4] Although they exhibit excellent luminescence properties, their instability towards moisture has limited their application in WLEDs.[5] Generally, the utilization of hydrophobic materials to coat phosphor surfaces could render phosphors more waterproof under high-humidity conditions. To minimize the reduction of the luminous efficacy, the coating layers should be optically transparent and homogeneously cover the surface of individual phosphor particles.[6] Metal oxide shells, such as SiO_2, TiO_2, SnO_2, Al_2O_3, Y_2O_3, and ZnO, are excellent moisture-resistant coatings for phosphors.[6–12] However, these coatings tend to decrease the luminous efficacy of phosphors. Coatings based on organic polymers have exhibited improved water tolerance and quantum efficiency but are not stable at high temperatures.[6,13] Organophosphate (OP, alkyl phosphate) materials have numerous industrial applications; for example, they are used as fire retardants, battery electrolytes, hardeners for film and photo materials, and as lubricants in engines operating at extremely high temperatures.[14–18] The application of self-assembled alkyl phosphate monolayers on metal or metal oxide surfaces as a means of stabilization has also been used for protein-adsorbed surfaces, dental-implant surfaces, passive metal surfaces, and the corrosion protection of interfaces.[19–23] Alkyl phosphates can be divided into three groups, namely monoalkyl phosphates $[OP(OH)_2(OR)]$, dialkyl phosphates $[OP(OH)(OR)_2]$, and trialkyl phosphates $[OP(OR)_3]$, all of which are prepared by the esterification of phosphoric acid with alcohols:[24]

$$OP(OH)_3 + ROH \rightarrow OP(OH)_2(OR) + H_2O \quad (1)$$

$$OP(OH)_2(OR) + ROH \rightarrow OP(OH)(OR)_2 + H_2O \quad (2)$$

$$OP(OH)(OR)_2 + ROH \rightarrow OP(OR)_3 + H_2O \quad (3)$$

The formation of alkyl phosphate films on substrates proceeds by an adsorption mechanism. Alkyl groups are partially displaced by breaking the P–O or C–O bond to yield a bound phosphate, which then reacts further to produce a polyphosphate film.[17,25–27] Currently, alkyl phosphate films are used as hydrophobic layers on indium–tin oxide particles, displaying a high optical transparency and electrical conductivity.[28] TiO_2 nanoparticles that were modified with oleyl phosphate through the formation of stable Ti–O–P bonds have been utilized to prepare poly(methyl methacrylate) based hybrid thin films with excellent optical transparency (refractive index, $n = 1.86$).[29]

Herein, we present a simple method for coating a hydrophobic alkyl phosphate layer onto the fluorosilicate phosphor $K_2SiF_6:Mn^{4+}$ (KSFM). Transition-metal ions (Zn^{2+}, Al^{3+}, Ti^{4+}) were used as cross-linkers between the alkyl phosphate groups through the formation of M–O–P–O–M bonds[30] to create a network on the substrate surface. The coated phosphors exhibited high emission intensity, excellent thermal stability, and high moisture resistance. The alkyl phosphate coated KSFM material is a potential candidate for stable-color warm WLEDs. A red KSFM phosphor was prepared following the two-step co-precipitation method.[3] The prepared KSFM was coated with a hydrophobic organophosphate (OP) layer through the esterification of phosphorus pentoxide (P_2O_5) with alcohols (methanol, ethanol, and isopropanol). The coatings are abbreviated as (M/E/I)OP(Zn/Al/Ti), with M, E, and I representing the alcohols methanol, ethanol, and isopropanol, respectively, and Zn, Al, and Ti are the metal ions acting as cross-linkers between the alkyl

[*] Dr. H.-D. Nguyen,[+] Dr. C. C. Lin,[+] Prof. Dr. R. S. Liu
Department of Chemistry, National Taiwan University
Taipei, 106 (Taiwan)
E-mail: rsliu@ntu.edu.tw
Prof. Dr. R. S. Liu
Department of Mechanical Engineering and Graduate Institute of Manufacturing Technology
National Taipei University of Technology
Taipei, 106 (Taiwan)
Dr. H.-D. Nguyen[+]
Institute of Applied Materials Science
Vietnam Academy of Science and Technology
Hochiminh City, 700000 (Vietnam)
[+] These authors contributed equally to this work.

Supporting information for this article is available on the WWW under http://dx.doi.org/10.1002/anie.201504791.

phosphate moieties. The formation of the alkyl phosphate layer on the phosphor surface is illustrated in Figure 1.

The X-ray diffraction (XRD) patterns of simple KSFM and KSFM coated with an OP layer using Al ions as the cross-linkers and different alkyl alcohols are shown in Figure 2 A.

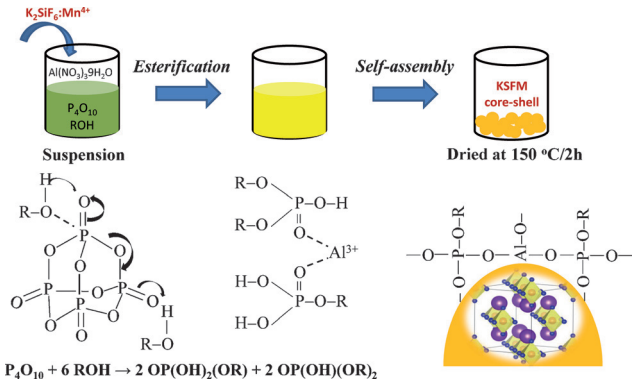

Figure 1. Formation of the alkyl phosphate layer on the phosphor surface.

All diffraction peaks can be indexed to the space group $D_3^2 - P321$ of the hexagonal K_2SiF_6 (JCPDS No. 0750694). Neither impurity phases nor second phases were observed for any of the coated samples. The Fourier transform infrared (FTIR) spectra of the KSFM samples prepared using either methanol, ethanol, or isopropanol showed bands at 1000–1100 cm^{-1}, which may be attributed to vibrations of the alkyl phosphates,[18,31] and bands at 2700–3000 cm^{-1}, which correspond to vibrations of the C–H groups (Figure 2 B).

Photoluminescence excitation (PLE) and photoluminescence (PL) spectra of uncoated and coated phosphors that were measured at room temperature are shown in Figure 2 C. When monitoring the emission at $\lambda_{em} = 620$ nm, the excitation spectrum exhibited two broad bands with peaks at approximately 460 and 360 nm, which are mainly due to the spin-allowed transitions of $^4A_{2g} \rightarrow {}^4T_{1g}$ and $^4A_{2g} \rightarrow {}^4T_{2g}$, respectively. The sharp red emission lines in the range of 600–650 nm are due to spin-forbidden $^2E_g \rightarrow {}^4A_{2g}$ transitions. The emission peaks at approximately 598, 609, 613, 619, 631, 635, and 647 nm are due to transitions of the ν_3 (t_{1u}), ν_4 (t_{1u}), ν_6 (t_{2u}), zero phonon line (ZPL), ν_6 (t_{2u}), ν_4 (t_{1u}), and ν_3 (t_{1u}) vibronic modes, respectively.[32,33] The relatively small decrease in the emission intensity of KSFM–MOPAl compared to that of KSFM is also illustrated in Figure 2 C. However, the emission intensities of the KSFM–EOPAl and KSFM–IOPAl samples were lower than those of KSFM–MOPAl and KSFM. Owing to the higher boiling points of isopropanol (82 °C) and ethanol (79 °C) compared to that of methanol (65 °C), different reaction temperatures (ca. 70, 60, and 50 °C) were used in the coating processes with isopropanol, ethanol, and methanol, respectively. The higher reaction temperatures might have an effect on the luminescence efficiency of the KSFM phosphors. The external quantum efficiencies (EQEs) of KSFM, KSFM–IOPAl, KSFM–EOPAl, and KSFM–MOPAl measured at room temperature were 0.556, 0.487, 0.495, and 0.549, respectively. The peaks corresponding to K, F, Si, Mn, O, Al, and P were clearly observed by energy-dispersive spectroscopy (EDS) of the coated samples prepared at an OP concentration of 0.01 M (Figure 3 A and B). The obtained P/Al weight ratio (ca. 2:1) closely matched the molar ratio of P_2O_5 to $Al(NO_3)_3$ (ca. 1:1) used in the preparation process. Field-emission scanning electron microscopy images (inset) show that the unmodified KSFM particles have a hexagonal shape whereas the coated particles are almost round; both are approximately 5–10 μm in diameter. The X-ray photoelectron spectra (XPS) depict the core elements K, Si, and F of the phosphor and the shell elements Al, P, O, and C of the OP coating layer (Figure 3 C). As expected, the atomic percentage of the shell elements increased as the OP concentration was increased from 0.01 M to 0.10 M (Figure 3 C). The very small increase in the Al percentage at high OP concentrations (0.10 M) indicates that the optimal concentration for the Al cross-linker is approximately 0.05 M. The mor-

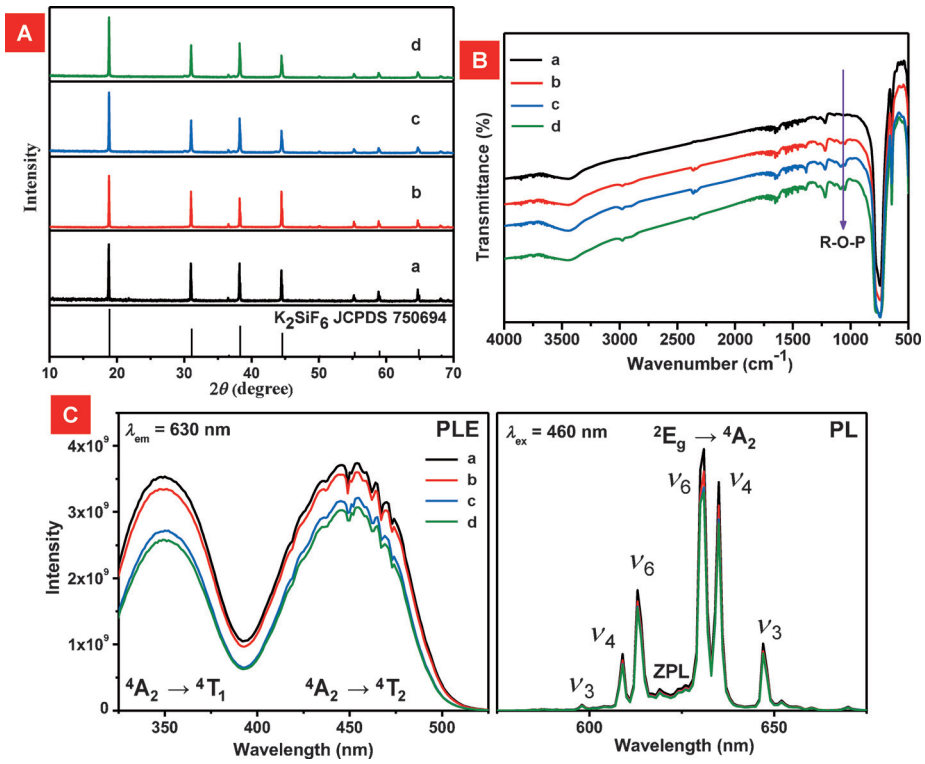

Figure 2. A) XRD patterns, B) FTIR spectra, and C) PLE and PL spectra of KSFM (a), KSFM–MOPAl (b), KSFM–EOPAl (c), and KSFM–IOPAl (d).

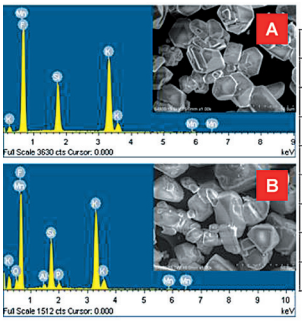

	KSFM		KSFM-MOPAl	
Element	Wt (%)	Atomic (%)	Wt (%)	Atomic(%)
O			6.74	9.51
K	26.81	15.76	25.76	14.88
Si	10.44	8.55	8.63	6.94
F	62.41	75.55	56.37	67.02
Mn	0.34	0.14	0.74	0.30
Al			0.6	0.50
P			1.16	0.85

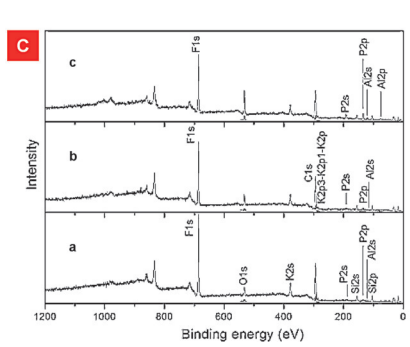

Average atomic (%)			
P2p	Al2p	C1s	O1s
6.85	1.25	3.50	26.15
2.35	1.15	3.40	12.35
0.85	0.45	2.80	8.10

Figure 3. EDS spectra of A) KSFM and B) KSFM–MOPAl. C) XPS spectra of KSFM–MOPAl coated with various OP concentrations: 0.01 M (a), 0.05 M (b), and 0.10 M (c).

phologies of KSFM–MOPAl phosphors prepared with various OP concentrations are shown in the Supporting Information, Figure S2.

Transmission electron microscopy (TEM) images of KSFM at different magnifications are shown in Figure 4 A and B. The high-resolution image shows that the KSFM surface decomposed under the electron beam of a TEM system (Figure 4 B), indicating the instability of the KSFM phosphors. TEM images of the coated samples show that the thickness of the coating layer on the KSFM surface increased from 50 to 100 nm as the OP concentration was increased from 0.01 to 0.10 M (Figure 4 C–E). Even at high magnification, no distortions of the surface of the coated sample were observed under electron irradiation.

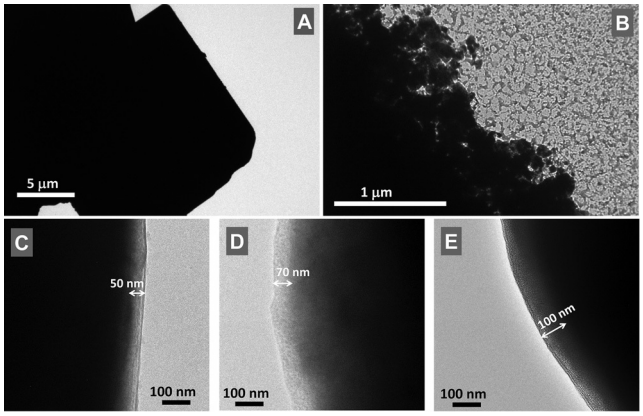

Figure 4. TEM images of KSFM (A and B) and KSFM–MOPAl samples with the coatings prepared at different concentrations: different coating layers: 0.01 M (C), 0.05 M (D), and 0.10 M (E).

An increase in the thickness of the coating led to a slight decrease in the PL intensity of the KSFM–MOPAl samples (Figure S3). EQE values of 0.549 (0.01 M OP), 0.517 (0.05 M OP), and 0.506 (0.10 M OP) were recorded for the coated samples, whereas that of KSFM was approximately 0.556. However, KSFM phosphors promptly decomposed in water (Figure S4). The yellowish color of the KSFM particles quickly turned brown after 30 min, whereas the KSFM–MOPAl sample was still yellow after 60 min in water. The water tolerance of samples prepared with various cross-linkers (MOPZn, MOPAl, and MOPTi) was also tested by measuring their PL in water (Figure S5). After 10, 30, and 60 min, the integrated luminescence intensity values ($I_{PL,t}/I_{PL,t=0}$) of the KSFM–MOPAl sample were 100, 80, and 50 %, respectively, whereas those of KSFM were approximately 50, 40, and 9 %, respectively (Figure S6). A KSFM–MOPAl sample showed significant durability when it was exposed to a hazardous environment with 85 % humidity and a temperature of 85 °C for 30 days (Figure 5 A, B). The relative internal quantum efficiency ($RIQE = IQE_t/IQE_{t=0}$) of approximately 85 % and the external quantum efficiency ($REQE = EQE_t/EQE_{t=0}$) of about 87 % of KSFM–MOPAl (0.05 M OP) were significantly higher than those of KSFM ($RIQE \approx 57\%$ and

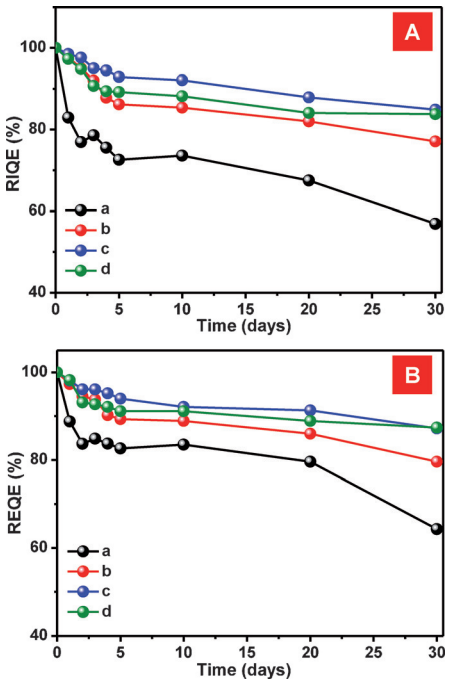

Figure 5. A) RIQE and B) REQE of KSFM–MOPAl samples prepared with various OP concentrations: 0.00 M (a), 0.01 M (b), 0.05 M (c), and 0.10 M (d). The IQE and EQE values of the samples were measured after aging under HH and HT conditions and 460 nm light irradiation.

$REQE \approx 64\%$) after 30 days under high-humidity (HH) and high-temperature (HT) conditions (Table S1). The slight decrease in the moisture resistance of a KSFM–MOPAl (0.10 M OP) sample kept under HH and HT conditions might have been caused by the increase in the organic content of the coating layer.

The room-temperature PL decay characteristics of the emitting ^2E_g state of the KSFM and KSFM–MOPAl samples are shown in Figure 6A. The PL decay time was determined

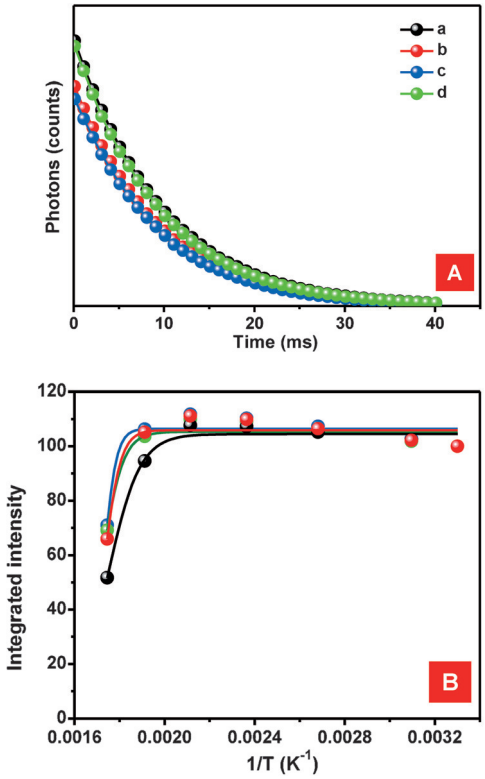

Figure 6. A) PL decay curves at 303 K and B) integrated red PL intensity as a function of temperature (303–573 K) for KSFM–MOPAl samples prepared with various OP concentrations: 0.00 M (a), 0.01 M (b), 0.05 M (c), and 0.10 M (d). The solid lines represent the result of fitting to the expression $I_T/I_0 = [1 + D\,e^{(-E_a/kT)}]^{-1}$.

on the basis of a single exponential fit. The PL lifetimes of KSFM, KSFM–MOPAl (0.01 M OP), KSFM–MOPAl (0.05 M OP), and KSFM–MOPAl (0.10 M OP) were determined to be 9.7, 9.3, 9.2, and 9.5 ms, respectively. These results indicate that the OP coating layers did not change the PL properties of the KSFM red phosphor.

The temperature-dependent emission spectra of various KSFM–MOPAl phosphors with different OP concentrations under 460 nm light excitation are shown in Figure S7. The temperature dependence of the integrated PL intensity (I_{PL}/I_{PL303}; Figure 6B) confirms the considerable stability of the KSFM–MOPAl particles in the temperature range of 303–573 K. Similar to that at 303 K, the relative PL intensity of KSFM–MOPAl at 523 K remained at 100%; and this phosphor thus clearly exhibits a better thermal stability than KSFM (94% at 523 K). The non-radiative transition probability increased with temperature, and the integrated PL intensity showed thermal quenching, which can be fitted to $I_T/I_0 = [1 + D\,e^{(-E_a/kT)}]^{-1}$, where I_0 is the intensity at $T = 0$ K while D and the activation energy E_a are the refined variables. An activation energy of 0.92 eV was obtained for KSFM–MOPAl, which is higher than that of KSFM (ca. 0.83 eV). This result corroborates the excellent thermal stability of the coated KSFM–MOPAl phosphors.

WLEDs that consisted of blue InGaN chips, commercially available yellow $Y_3Al_5O_{12}:Ce^{3+}$ (YAG) phosphors or green β-SiAlON:Eu^{2+} phosphors, and red KSFM or KSFM–MOPAl phosphors were then fabricated. A high-performance warm WLED with a high color rendering index (CRI; $R_a = 86$, $R9 = 93$) and a luminous efficacy of 79 Lm W^{-1} was obtained when YAG and KSFM–MOPAl were employed. The chromaticity coordinates [(0.4169, 0.4244), (0.3995, 0.4091), and (0.3748, 0.3587)] were near the black body locus according to the color spaces of the 1931 Commission Internationale de l'Éclairage (CIE). Correlated color temperatures (CCTs) of 3519 K, 3766 K, and 4024 K were measured for WLEDs consisting of YAG and KSFM, YAG and KSFM–MOPAl, and β-SiAlON and KSFM–MOPAl, respectively (Figure S8). The CCT, CRI, and efficacy values of these WLEDs are summarized in Table 1.

Table 1: Photoelectric parameters for three WLEDs with different CCTs.

White LED	CCT [K]	Efficacy [Lm W^{-1}]	R_a	R9
YAG and KSFM	3519	82	86	87
YAG and KSFM–MOPAl	3766	79	86	93
β-SiAlON and KSFM–MOPAl	4024	67	80	69

The electroluminescence spectra of the warm WLEDs are presented in Figure S9. The moisture resistance values of warm WLEDs based on β-SiALON with commercially available KSFM (WLED/cKSFM), prepared KSFM (WLED/pKSFM), KSFM–MOPAl (WLED/coatedKSFM), and β-SiALON were also obtained. After 2016 h under HH and HT conditions with continuous application of a voltage of 120 mA, the relative quantum efficiency of WLED/cKSFM had decreased more strongly (to ca. 40% of the initial intensity) than that of WLED/pKSFM (ca. 60% of the initial intensity). WLED/coatedKSFM demonstrated excellent waterproof properties, retaining 86% of its initial quantum efficiency (Figure S10). The estimated WLED lifetimes are shown in Figure S11. The optical intensities of WLED/cKSFM, WLED/pKSFM, and WLED/coatedKSFM reached 50% of their original values after 3660, 4627, and 8159 h, respectively, under HH and HT conditions. The high thermal stability and waterproof properties under HH and HT conditions indicate that the alkyl phosphate coated KSFM particles are promising red phosphors for warm WLED applications.

In conclusion, KSFM red fluoride phosphors with and without a coating alkyl phosphate layer were synthesized by a simple method. No impurities or other fluoride phases were detected in the coated samples. The luminescence intensities of the coated phosphors slightly decreased as the shell thickness increased. KSFM–MOPAl phosphors exhibited low thermal quenching and excellent moisture resistance, as well as an integrated PL intensity of approximately 100% at 523 K and a relative external quantum efficiency of approximately 87% after one month under HH and HT conditions. Approximately 86% of the luminous efficacy of the WLED/

coatedKSFM material was also retained after it had been subjected to a continuous current (120 mA) under HH and HT conditions for 2016 hours. The efficient red luminescence under blue-light excitation, low thermal quenching, and high humidity stability of the coated KSFM particles show that alkyl phosphate materials are potential candidates for optoelectronic applications.

Experimental Section

Hydrofluoric acid (HF, 48%), aluminum nitrate nonahydrate ($Al(NO_3)_3{\cdot}H_2O$, $\geq$98%), phosphorus pentoxide (P_2O_5, 99%), hydrogen peroxide solution (H_2O_2, 30 wt% in H_2O), methanol, ethanol, isopropanol, and acetone (99.9%) were purchased from Sigma–Aldrich. Zinc nitrate hexahydrate ($Zn(NO_3)_2{\cdot}6H_2O$, 99.9%), titanium(IV) butoxide [$Ti(OBu)_4$, 99%], potassium hydrogen fluoride (KHF_2, 99%), potassium fluoride (KF, 99%), and potassium permanganate ($KMNO_4$, 99%) were obtained from Alfa Aesar and Baker Analyzed. K_2MnF_6 was prepared by dissolving a mixture of KHF_2 (9.0 g) and $KMnO_4$ (0.45 g) in 30 mL of a 48% HF solution. Then, H_2O_2 (0.3 mL, 35–40%) was added to the solution by using a dropper. The deep-purple solution gradually turned yellow, and a yellow precipitate was obtained. The K_2MnF_6 powder was washed with acetone several times and dried at 70°C for 2 h. The K_2MnF_6 powder (0.3 g) was dissolved in a solution of SiO_2 (1.2 g) in 48% HF (35 mL) by stirring. Subsequently, KF (3.5 g) was added slowly to the solution while stirring for 15 min. A yellow $K_2SiF_6{:}Mn^{4+}$ powder was obtained, washed with 20% HF solution and acetone, and dried at 70°C for 6 h. The prepared KSFM was coated with a hydrophobic organophosphate (OP) through the esterification of P_2O_5 and alcohols. Exactly 0.5 g of the KSFM powder was dispersed in an OP solution of the alcohol, P_2O_5, and cross-linkers [$Zn(NO_3)_2$, $Al(NO_3)_3$, or $Ti(OBu)_4$]. P_2O_5 and the cross-linkers were used in a molar ratio of 1:1. P_2O_5 and cross-linker concentrations (OP concentration) of 0.01 M to 0.10 M were used. The suspension was evaporated at 50–70°C. The obtained powder was washed with alcohol and acetone before final heating at 150°C for 2 h.

Acknowledgements

We thank the Ministry of Science and Technology of Taiwan (MOST 101-2113M-002-014-MY3). We thank Leo Yeh for carrying out the reliability test of the LED devices at Unity Opto Technology Co., Ltd.

Keywords: light-emitting diodes · phosphors · photoluminescence · white light

How to cite: *Angew. Chem. Int. Ed.* **2015**, *54*, 10862–10866
Angew. Chem. **2015**, *127*, 11012–11016

[1] S. Adachi, H. Abe, R. Kasa, T. Arai, *J. Electrochem. Soc.* **2012**, *159*, J34.
[2] H. M. Zhu, C. C. Lin, W. Luo, S. T. Shu, Z. G. Liu, M. Wang, J. T. Kong, E. Ma, Y. Cao, R. S. Liu, X. Y. Chen, *Nat. Commun.* **2014**, *5*, 4312.
[3] H.-D. Nguyen, C. C. Lin, M.-H. Fang, R.-S. Liu, *J. Mater. Chem. C* **2014**, *2*, 10268.
[4] M. Kim, W. B. Park, B. Bang, C. H. Kim, K.-S. Sohn, *J. Mater. Chem. C* **2015**, *3*, 5484.
[5] B. Wang, H. Lin, J. Xu, H. Chen, Y. Wang, *ACS Appl. Mater. Interfaces* **2014**, *6*, 22905.
[6] J. Zhuang, Z. Xia, H. Liu, Z. Zhang, L. Liao, *Appl. Surf. Sci.* **2011**, *257*, 4350.
[7] J. Sun, R. Sun, H. Du, *Appl. Surf. Sci.* **2012**, *258*, 4569.
[8] M. K. Mishra, S. Chattopadhyay, A. Mitra, G. De, *Ind. Eng. Chem. Res.* **2015**, *54*, 928.
[9] C. Zhang, T. Uchikoshi, L. Liu, Y. Sakka, N. Hirosaki, *Materials* **2014**, *7*, 3623.
[10] J.-H. Seo, S.-M. Lee, H.-S. Moon, S.-J. Han, S.-H. Sohn, *Mol. Cryst. Liq. Cryst.* **2010**, *531*, 82.
[11] W. Park, K. Yasuda, B. K. Wagner, C. J. Summers, Y. R. Do, H. G. Yang, *Mater. Sci. Eng. B* **2000**, *76*, 122.
[12] H.-H. Choi, M. Ollinger, R. K. Singh, *Appl. Phys. Lett.* **2003**, *82*, 2494.
[13] T. Chen, Y. Luo, J. Zou, L. Jiang, Y. Dan, L. Zhang, K. Zhao, *J. Appl. Polym. Sci.* **2008**, *109*, 3811.
[14] P. Moy, *J. Vinyl Addit. Technol.* **2004**, *10*, 187.
[15] O. Borodin, W. Behl, T. R. Jow, *J. Phys. Chem. C* **2013**, *117*, 8661.
[16] D. Sung, A. J. Gellman, *Tribol. Int.* **2002**, *35*, 579.
[17] D. W. Johnson, J. E. Hils, *Lubricants* **2013**, *1*, 132.
[18] I. N. Smirnova, A. Cuisset, F. Hindle, G. Mouret, R. Bocquet, O. Pirali, P. Roy, *J. Phys. Chem. B* **2010**, *114*, 16936.
[19] R. Hofer, M. Textor, N. D. Spencer, *Langmuir* **2001**, *17*, 4014.
[20] R. Michel, J. W. Lussi, G. Csucs, I. Reviakine, G. Danuser, B. Ketterer, J. A. Hubbell, M. Textor, N. D. Spence, *Langmuir* **2002**, *18*, 3281.
[21] A. Paszternák, S. Stichleutner, I. Felhősi, Z. Keresztes, F. Nagyb, E. Kuzmannb, A. Vértes, Z. Homonnay, G. Pető, E. Kálmán, *Electrochim. Acta* **2007**, *52*, 337.
[22] J. Wu, I. Hirata, X. Zhao, B. Gao, M. Okazaki, K. Kato, *J. Biomed. Mater. Res. Part A* **2013**, *101*, 2258.
[23] M. F. Sonnenschein, C. M. Cheatham, *Langmuir* **2002**, *18*, 3578.
[24] C. Dueymes, C. Pirat, R. Pascal, *Tetrahedron Lett.* **2008**, *49*, 5300.
[25] D. W. Johnson, S. Morrow, *Chem. Mater.* **2002**, *14*, 3767.
[26] M. J. Pellerite, T. D. Dunbar, L. D. Boardman, E. J. Wood, *J. Phys. Chem. B* **2003**, *107*, 11726.
[27] S. Pawsey, K. Yach, L. Reven, *Langmuir* **2002**, *18*, 5205.
[28] C. S. Tang, M. Antoni, I. Schönbächler, B. Keller, M. Textor, J. Vörös, *ECS Trans.* **2006**, *1*, 29.
[29] M. Fujita, N. Idota, K. Matsukawa, Y. Sugahara, *J. Nanomaterials* **2015**, 297197.
[30] A. Clearfield, *Curr. Opin. Solid State Mater. Sci.* **2002**, *6*, 495.
[31] D. F. Peppard, J. R. Ferraro, G. W. Mason, *J. Inorg. Nucl. Chem.* **1961**, *16*, 246.
[32] Y. Tanabe, S. Sugano, *J. Phys. Soc. Jpn.* **1954**, *9*, 753.
[33] R. Kasa, S. Adachi, *J. Electrochem. Soc.* **2012**, *159*, J89.

Received: May 27, 2015
Published online: July 23, 2015

